Journal of the Oceanographical Society of Japan
Vol. 32, pp. 271 to 283, 1976

The Wind Field over Wind-waves*

Hiroshi ICHIKAWA** and Norihisa IMASATO**

Abstract: The velocity fluctuations of wind over wind-waves in a wind tunnel are measured with a X-type hot-wire anemometer at some heights over the water surface.

The observed vertical profiles of the wave-induced velocity fluctuations and the wave-induced Reynolds stress at the wave spectral peak frequency are different from those expected from the inviscid quasi-laminar model; *i.e.*, the observed vertical profiles of the power spectral density of the wave-induced horizontal or vertical velocity fluctuations of wind have the minimum value at the height much heigher than the critical layer, and the value of the wave-induced Reynolds stress is negative at several heights over the water surface. From the comparison between the experimental results and the numerical solutions of a linear model of the turbulent shear flow over the wavy boundary, it is shown that the discrepancy described above can be attributed to the atmospheric turbulence.

1. Introduction

In order to understand the mechanism of the development of wind-waves, many investigators have performed a large number of field observations and laboratory experiments, and many informations on the wind-wave phenomena have been accumulated.

MILES (1957) theoretically studied this problem, and found that the momentum of the air flow was transferred from the critical layer to wind-waves. LIGHTHILL (1962) gave the physical interpretation to the Miles' model. Their studies seemed to have solved the problem of the wind-wave development, but SNYDER and COX (1966) and BARNETT and WILKERSON (1967) found that the growth rate of wind-waves observed in the ocean was much greater than that expected from the Miles' model.

One of the authors performed some wind tunnel experiments and field observations (IMASATO, 1976a), and he concluded that the dominant wind-wave spectral peak, which is the steepest wave in the spectrum, receives the momentum from the air flow according to the Miles' (1957, 1962) mechanism and nonlinearly transports the wave energy to the forward face and to the high frequency part in the wave spectrum (IMASATO, 1976b).

HASSELMANN *et al.* (1973) concluded from the JONSWAP-observations that the shape of the wind-wave spectrum is determined by the nonlinear energy transfer from the central region of the spectrum to both shorter and longer wave components.

On the other hand, motivated by Miles' (1957) study using the quasi-laminar model, several investigators tried to clarify the actual features of the wave-induced fluctuations of wind and those of the wave-induced Reynolds stress in the boundary layer over the wavy surface.

PHILLIPS (1966) suggested that the wave-induced variations of turbulent Reynolds stresses, which were neglected by MILES, play some role in the momentum transfer from wind to wind-waves. YEFIMOV (1970), REYNOLDS and HUSSAIN (1972), DAVIS (1970, 1972) and TOWNSEND (1972) theoretically investigated the effects of the atmospheric turbulence over the wavy boundary.

STEWART (1970), LAI and SHEMDIN (1971) and KATO and SANO (1971) measured the wave-induced fluctuations of wind over the regular wave produced by a wave generator in the wind tunnels. STEWART (1970) compared the experimental results with the numerical solutions of linear equations governing the shearing flow over the wavy water surface, and concluded

* Received Dec. 18, 1975, revised and accepted Aug. 31, 1976.

** Geophysical Institute, Faculty of Science, Kyoto University, Kitashirakawa Oiwake-cho, Sakyo-ku, Kyoto, 606 Japan

that the atmospheric turbulence plays an important role in the momentum transfer from wind to wind-waves.

The turbulent fluctuations of wind over the the regular wave are fairly small to discuss the effects of the atmospheric turbulence on the momentum transfer to the wind-waves. The air flow over the irregular wind-waves is much more turbulent than that over the regular wave because of the large steepness of the wind-wave field. Therefore, the atmospheric turbulence will play much more important role in the momentum transfer from the air flow to the irregular wind-waves, which we intend to discuss in this paper.

We performed a wind tunnel experiment and numerical calculations in order to clarify the characteristics of the turbulent air flow over the irregular wind-waves. In this paper, we will discuss the vertical change of the wave-induced Reynolds stress and the wave-induced fluctuations of wind obtained from the wind tunnel experiment and the numerical solutions of the viscous Orr-Sommerfeld equation. In the theoretical model about the turbulent shear flow over the wavy boundary, the atmospheric turbulence is taken into account in the form of the eddy viscosity.

2. Wind tunnel experiment and the evaluation of the wave-induced wind fluctuations

The wind tunnel, used in this experiment, is 80 cm in width, 130 cm in height, 40 m in length and 1 m in water depth. The range of the wind speed used in this experiment is from 2.1 to 8.9 m s^{-1} at the central core of the wind tunnel.

The water surface displacements were measured by the capacitance-type wave gauge. The horizontal and vertical velocity fluctuations of wind were measured by a X-type hot-wire anemometer at several heights in the boundary layer over the wave crests. This hot-wire anemometer was calibrated before and after the every run of the experiment by using an ultrasonic anemometer. The hot-wire anemometer was located at a distance of 8 cm in parallel with wave gauge, so that the wind-waves and the velocity fluctuations of wind over the wind-waves could be measured at the same fetch of 19 m.

Signals of these fluctuations were digitalized at an adequate interval, and the power and cross spectra were computed by the correlation method of BLACKMAN and TUKEY (1958). The degree of freedom of spectra is fourty-five.

In order to investigate the momentum transfer from wind to wind-waves and the mechanism of the development of wind-waves, it is necessary to understand the structures of the wind field over the irregular wind-waves, especially the wave-induced wind fluctuations. Therefore, we must separately evaluate the wave-induced fluctuations of wind from the fluctuations of wind measured by a hot-wire anemometer. This separation was performed on the assumptions as is described in the following.

The measured horizontal velocity fluctuations of wind u over the wavy boundary are represented as

$$u=\tilde{u}+u' \tag{2.1}$$

where $\tilde{u}$ is the velocity fluctuations coherent to wind-waves or the wave-induced fluctuations and u' is the turbulent fluctuations noncoherent to wind-waves. As $\tilde{u}$ and u' are noncoherent each other, the power spectral density $S_u(f)$ of u is equal to the sum of power spectral densities $S_{\tilde{u}}(f)$ and $S_{u'}(f)$ of the velocity fluctuations $\tilde{u}$ and u', respectively, where f is the frequency. Because the turbulent fluctuations of wind u' and the water surface displacement ζ are noncoherent each other by the definition, the cross-spectral density $X_{u\zeta}(f)$ between u and ζ equals the cross-spectral density $X_{\tilde{u}\zeta}(f)$ between $\tilde{u}$ and ζ, *i.e.*,

$$X_{u\zeta}(f)=X_{\tilde{u}\zeta}(f) \tag{2.2}$$

The coherence $r^2_{u\zeta}(f)$ between u and ζ and the coherence $r^2_{\tilde{u}\zeta}(f)$ between $\tilde{u}$ and ζ are defined as

$$r^2_{u\zeta}(f)=\frac{|X_{u\zeta}(f)|^2}{S_u(f)S_\zeta(f)} \tag{2.3}$$

$$r^2_{\tilde{u}\zeta}(f)=\frac{|X_{\tilde{u}\zeta}(f)|^2}{S_{\tilde{u}}(f)S_\zeta(f)} \tag{2.4}$$

where $S_\zeta(f)$ is the power spectral density of wind-waves. Owing to the definition, the coherence $r^2_{\tilde{u}\zeta}(f)$ is found to be equal to unity. Therefore, if any noise is not contained in the

present system, the power spectral density $S_u(f)$ can be separated into the spectral densities $S_{\tilde{u}}(f)$ and $S_{u'}(f)$ as follows:

$$S_{\tilde{u}}(f)=r^2_{u\zeta}(f)\,S_u(f) \qquad (2.5)$$

$$S_{u'}(f)=(1-r^2_{u\zeta}(f))\,S_u(f) \qquad (2.6)$$

Using the Eq. (2.2), we can find that the phase-difference $\theta_{u\zeta}(f)$ of the velocity fluctuations of wind u from the water surface displacements ζ is equal to the phase-difference $\theta_{\tilde{u}\zeta}(f)$ of $\tilde{u}$ from ζ. And the confidence limit of the phase-difference depends on the coherence between u and ζ (MUNK and CARTWRIGHT, 1960). The power spectral density $S_{\tilde{w}}(f)$ of the wave-induced vertical fluctuations of wind $\tilde{w}$ can be estimated by the same method as that for $\tilde{u}$. The symbols used for the various spectra in this section will be used also in the following sections without explanation.

3. Experimental results and discussion

Vertical profiles of the mean wind velocity in Run-I, II and III are shown in Fig. 1. They are found from this figure to follow the logarithmic law in the boundary layer over the wind-waves. The mean wind speeds in the central core of the wind tunnel were 2.1, 5.3 and 8.9 m s^{-1}, respectively for these three cases.

The friction velocity u_*, obtained from the logarithmic profiles, and the mean characteristic properties of the wind-wave field are shown in Table 1. From this table, it is clearly found that the critical layer corresponding to the dominant component wave, where the mean wind velocity is equal to the phase velocity of the dominant component wave, is situated at the lower level than that of the wave crests. Therefore, in this experiment, the wind velocity fluctuations in the neighbourhood of the critical layer corresponding to the component wave of the wave spectral peak could not be directly measured, because the wind velocity fluctuations must be measured at some levels higher than the wave crests.

The wind-wave spectrum of Run-I belongs to the stage of "transition stage", defined by IMASATO (1976a). The wind-wave spectra of Run-II and III belong to the stage of "sea-waves".

Table 1. Wave data and conditions relating to the spectral analysis.

		Run-I	Run-II	Run-III
U	(m s^{-1})	2.1	5.3	8.9
u_*	(cm s^{-1})	9.39	23.0	43.3
Mean amplitude	(cm)	0.132	0.840	1.74
Mean frequency	(Hz)	3.64	2.35	1.93
Wave number	(cm^{-1})	0.524	0.258	0.149
Critical height	(cm)	0.000309	0.00683	0.00256
u_*/c		0.214	0.346	0.533
Nyquist frequency	(Hz)	20.0	10.0	10.0
Lag number		100	100	100

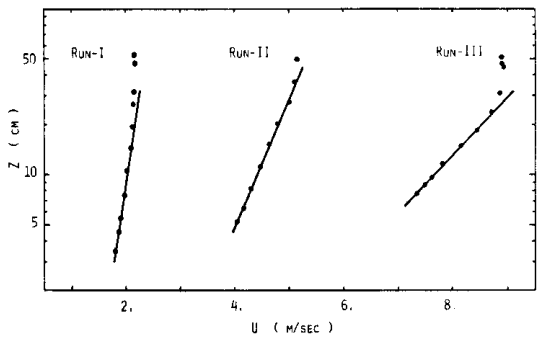

Fig. 1. Vertical profiles of the mean wind velocity.

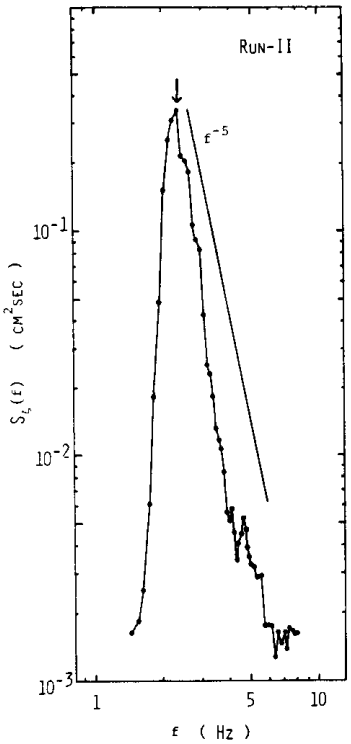

Fig. 2. Power spectrum $S_\zeta(f)$ of wind-waves in Run-II.

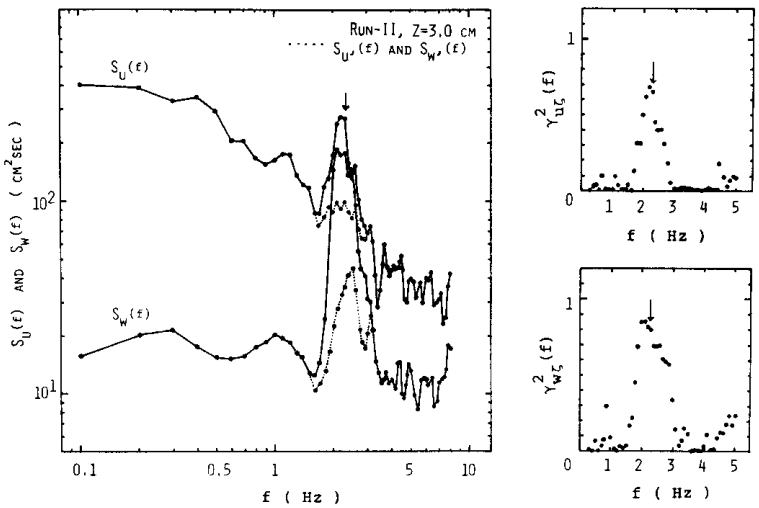

Fig. 3. Power spectra $S_u(f)$ and $S_w(f)$, and coherence spectra $\gamma^2 u\zeta(f)$ and $\gamma^2 w\zeta(f)$ at $Z=3.0$ cm in Run-II. The dotted lines represent the power spectra $S_{u'}(f)$ and $S_{w'}(f)$ obtained by the Eq. (2.6).

The power spectrum $S_\zeta(f)$ of wind-waves in the case of Run-II is shown in Fig. 2, in which the spectral peak is shown by an arrow. The high frequency part of $S_\zeta(f)$ does not follow the f^{-5} law proposed by PHILLIPS (1958), and decreases more rapidly with the frequency. This wave spectral form in the wind tunnel experiment has been well known (IMASATO, 1976a). IMASATO (1976b) showed that this wind-wave spectral form can be explained by the "momentum transfer filter" on the momentum transfer from wind to wind-waves and the nonlinear wave-wave interaction, and also by the fact that the upper limit of the development of the power spectrum $S_\zeta(f)$ is given by a certain ultimate value in the slope spectrum of wind-waves.

Fig. 3 shows the spectra $S_u(f)$, $S_w(f)$, $\gamma^2_{u\zeta}(f)$ and $\gamma^2_{w\zeta}(f)$ of Run-II, which were calculated from the time series of the water surface displacement ζ and the horizontal and vertical velocity fluctuations of the wind u and w measured at the height $Z=3.0$ cm ($Z=0$ indicates the mean water surface level). Each of the spectra $S_u(f)$, $S_w(f)$, $\gamma^2_{u\zeta}(f)$ and $\gamma^2_{w\zeta}(f)$ has a dominant peak near the frequency f_p of the wave spectral peak.

The peak of the power spectra $S_u(f)$ and $S_w(f)$ becomes obscure and the coherences $\gamma^2_{u\zeta}(f)$ and $\gamma^2_{w\zeta}(f)$ become smaller with increasing the height, where u and w were measured. At the sufficiently large height, the wind velocity fluctuations have the same characteristics as the ordinal atmospheric turbulence and the coherence between the velocity fluctuations of wind and the wind-waves is lost. The peak may be attributed to the wave-induced velocity fluctuations over the wind-waves.

The dotted curves in Fig. 3 represent the power spectra $S_{u'}(f)$ and $S_{w'}(f)$ obtained from the Eq. (2.6). These power spectra have the characteristics very similar to the atmospheric turbulence except that each of them has a weak peak near the frequency f_p. One possibility to explain this weak peak is to consider it to be the result of energy transfer from the wave-induced velocity fluctuations to the atmospheric turbulence.

We will compare the experimental vertical changes of the power spectral densities of $\tilde{u}$ and $\tilde{w}$ with the theoretical ones predicted by PHILLIPS (1966). The wind and the wind-wave fields in the wind tunnel may be considered to be in a steady state. There is, however, a few possibility to bring some errors into the evaluation of the vertical profile of the power spectral densities of $\tilde{u}$ and $\tilde{w}$, because it has been unable to measure the wind fluctuations simultaneously at several heights. Therefore, we will introduce the non-dimensional power spectra $\sigma^2_{\tilde{u}}$ and $\sigma^2_{\tilde{w}}$, which are non-dimensionalized with power spectrum $S_\zeta(f)$ of wind-waves measured simultaneously with the velocity fluctuations of

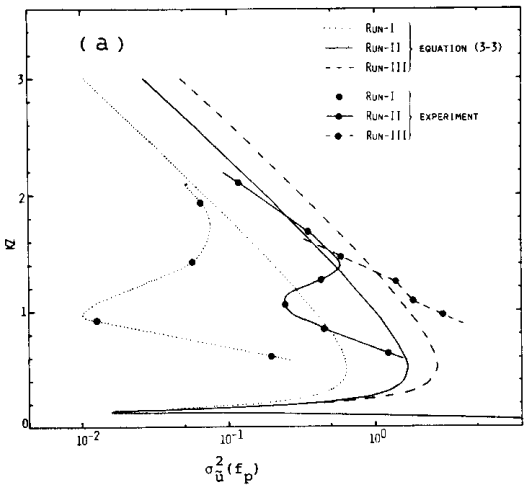

Fig. 4a. Vertical profiles of observed and theoretical value of $\sigma_{\tilde{u}}^2(f_p)$. K is the wave number corresponding to the component wave at the spectral peak.

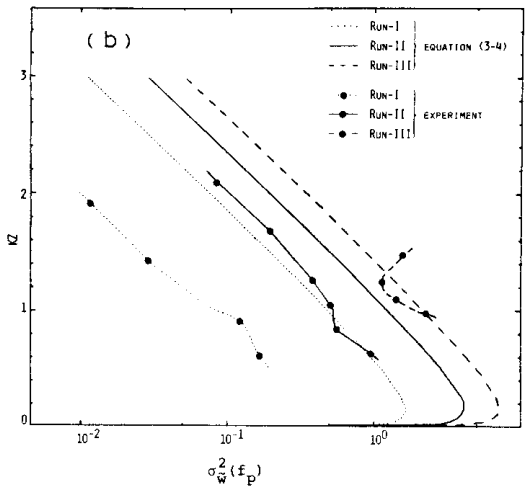

Fig. 4b. Vertical profiles of observed and theoretical value of $\sigma_{\tilde{w}}^2(f_p)$.

wind u and w, *i.e.*,

$$\sigma^2_{\tilde{u}}(f)=\frac{S_{\tilde{u}}(f)}{2(2\pi f)^2 S_\zeta(f)} \tag{3.1}$$

$$\sigma^2_{\tilde{w}}(f)=\frac{S_{\tilde{w}}(f)}{2(2\pi f)^2 S_\zeta(f)} \tag{3.2}$$

On the other hand, the theoretical non-dimensional spectra of $\tilde{u}$ and $\tilde{w}$ are given after PHILLIPS (1966) as follows:

$$\sigma^2_{\tilde{u}}(f)=\frac{\Gamma^2}{2}\left(\frac{U}{C}-\frac{U'}{KC}-1\right)^2\exp(-2KZ) \tag{3.3}$$

$$\sigma^2_{\tilde{w}}(f)=\frac{\Gamma^2}{2}\left(\frac{U}{C}-1\right)^2\exp(-2KZ) \tag{3.4}$$

where U is the mean wind velocity, C the phase velocity of the component wave of the frequency f, K the wave number and Γ^2 is given as

$$\Gamma^2=\begin{cases}1 & Z<Z_m\\ 1/3 & Z>Z_m\end{cases} \tag{3.5}$$

Z_m being the height of the critical layer corresponding to the component wave of the frequency f.

The observed spectral densities $\sigma^2_{\tilde{u}}(f)$ and $\sigma^2_{\tilde{w}}(f)$ of Run-I, II and III and the theoretical spectral densities, given by the Eqs. (3.3) and (3.4), are evaluated at the frequency f_p of the wave spectral peak and are shown in Fig. 4. It is seen from this figure that the observed profiles have the minimum value at the height much higher than the critical layer and they differ from the theoretical profiles. This disagreement between the theory and the experiment may be attributed to the effects of the atmospheric turbulence neglected in the Eqs. (3.3) and (3.4). Discussion about it will be given in the next section.

The wave-induced Reynolds stress is evaluated from the co-spectrum $C_{uw}(f)$ which represents the spectral distribution of the total Reynolds stress. The total Reynolds stress over wind-waves is the sum of the wave-induced Reynolds stress and the turbulent Reynolds stress. If the co-spectrum $C_{u'w'}(f)$ of the turbulent velocity fluctuations of wind over wind-waves can be evaluated by some ways, the frequency spectrum of the wave-induced Reynolds stress $-C_{\tilde{u}\tilde{w}}(f)$ can be given as follows:

$$-C_{\tilde{u}\tilde{w}}(f)=-C_{uw}(f)+C_{u'w'}(f) \tag{3.6}$$

The non-dimensional spectrum $T_1(f)$ of the wave-induced Reynolds stress given by Eq. (3.6) is expressed as

$$T_1(f)=\frac{-C_{\tilde{u}\tilde{w}}(f)}{2(2\pi f)^2 S_\zeta(f)} \tag{3.7}$$

The spectral distribution of the turbulent

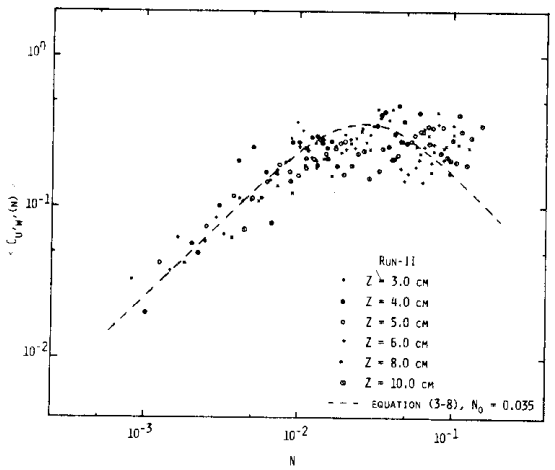

Fig. 5. Normalized co-spectra $\langle C_{uw}(n)\rangle$, in Run-II, in the frequency region except the narrow frequency band arround the wave spectral peak. The broken line represents the co-spectrum $\langle C_{u'w'}(n)\rangle$ given by the Eq. (3.8) with the parameter n_0 of 0.035.

Reynolds stress over wind-waves has not been well understood yet. On the other hand, the spectral distribution of the turbulent Reynolds stress over the solid wall boundary has been investigated by KAIMAL *et al.* (1973). They represented the normalized co-spectrum $\langle C_{u'w'}(n)\rangle$ of the turbulent velocity fluctuations of wind over the solid wall boundary as

$$\langle C_{u'w'}(n)\rangle = \frac{-fC_{u'w'}(f)}{-\overline{u'w'}} = \frac{0.88(n/n_0)}{1+1.5(n/n_0)^{2.1}} \qquad (3.8)$$

$$n = \frac{fZ}{U}$$

where Z is the height above the wall surface, U the mean wind velocity at Z, n the non-dimensional frequency, and n_0 a non-dimensional parameter.

From our experimental result that the wave-induced fluctuations of wind is concentrated in a narrow frequency band around the wave spectral peak, it can be considered that the co-spectrum $C_{uw}(f)$ represents the co-spectrum $C_{u'w'}(f)$ in the frequency regions except in the narrow frequency band around the wave spectral peak. Fig. 5 shows some examples of the normalized co-spectra $\langle C_{uw}(n)\rangle$ in the frequency regions except in the narrow frequency band around the wave spectral peak, measured at several heights in Run-II of our wind tunnel experiment. The normalized co-spectrum $\langle C_{u'w'}(n)\rangle$, given by the Eq. (3.8) with the parameter n_0 of 0.035, is shown by a broken line in this figure.

Although the observed normalized co-spectra $\langle C_{uw}(n)\rangle$ is rather scattered, especially in the high frequency region, it is seen from this figure that the normalized co-spectrum $\langle C_{u'w'}(n)\rangle$ between u' and w' over wind-waves can be given by the Eq. (3.8). Therefore, the co-spectrum $C_{u'w'}(f)$ over wind-waves is represented as

$$-C_{u'w'}(f) = -\overline{\tilde{u}\tilde{w}}\,\frac{n}{f}\,\frac{0.88\,n_0^{-1}}{1+1.5(n/n_0)^{2.1}} \qquad (3.9)$$

where the value of the parameter n_0 is taken to be 0.025, 0.035 and 0.050 respectively for Run-I, II and III of our experiment. The co-spectrum $-C_{\tilde{u}\tilde{w}}(f)$ between $\tilde{u}$ and $\tilde{w}$ can be evaluated using the Eqs. (3.6) and (3.9) in the fairly narrow frequency region around the wave spectral peak.

KAIMAL *et al.* (1973) concluded that the most suitable value of the parameter n_0 is 0.1 for the shearing flow in the neutral condition over the solid boundary. This discrepancy may be attributed to the surface condition; *i.e.*, in the present case of the wind tunnel experiment, momentum and energy are transferred to the water across the irregularly wavy surface, but, on the other hand, in Kaimal's measurements over the land, they are not transferred across the surface.

Fig. 6 shows the co-spectra $-C_{u'w'}(f)$ from the Eq. (3.9) and $-C_{\tilde{u}\tilde{w}}(f)$ from the Eqs. (3.6) and (3.9), and the phase spectra $\theta_{uw}(f)$ at Z=3.0, 5.0 and 8.0 cm in Run-II. It is found from this figure that the phase-difference between the velocity fluctuations u and w is nearly 180° outside the frequency region around the wave spectral peak. This fact indicats the characteristics of the turbulent velocity fluctuations of wind in the turbulent shear flow. On the other hand, in the frequency region around the wave spectral peak, the phase-difference shifts significantly from 180°, and it is attributed to the wave-induced fluctuations of wind.

The non-dimensional spectrum of the wave-

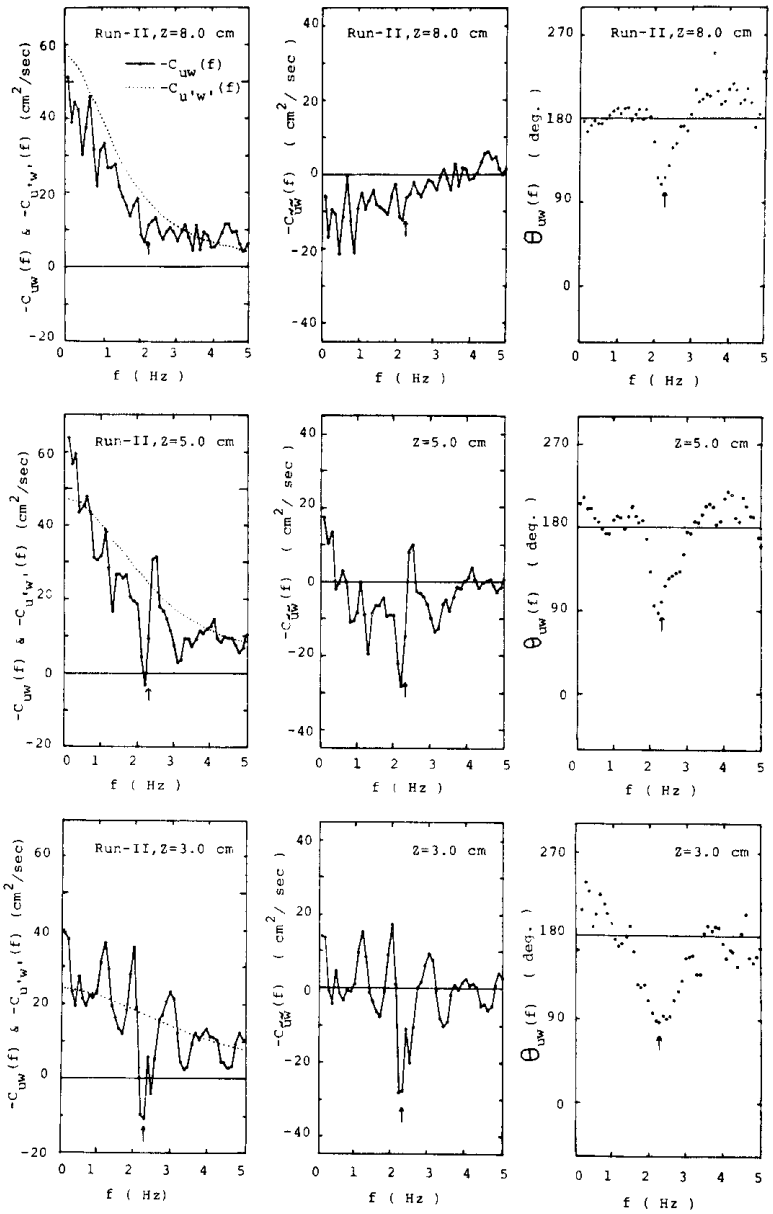

Fig. 6. Co-spectra $-C_{uw}(f)$ and $-C_{\tilde{u}\tilde{w}}(f)$, and phase-difference spectra $\theta_{uw}(f)$ at $Z=3.0$, 5.0 and 8.0 cm in Run-II. The dotted lines represent the co-spectra $-C_{u'w'}(f)$ given by the Eq. (3.9). $-C_{\tilde{u}\tilde{w}}(f)$ is evaluated by the Eq. (3.6). The frequency of the wave spectral peak is shown by arrows.

induced Reynolds stress is also given by the other method using the non-dimensional power spectral densities $\sigma^2_{\tilde{u}}(f)$ and $\sigma^2_{\tilde{w}}(f)$, and the phase-differences $\theta_{\tilde{u}\zeta}(f)$ and $\theta_{\tilde{w}\zeta}(f)$ between the wind-wave and the wave-induced fluctuations of wind. These phase-differences are equal to the observed phase-differences $\theta_{u\zeta}(f)$ and $\theta_{w\zeta}(f)$.

The non-dimensional spectrum $T_2(f)$ of the wave-induced Reynolds stress estimated by this method is given as

$$T_2(f)=-2(\sigma^2_{\tilde{u}}(f)\,\sigma^2_{\tilde{w}}(f))^{1/2} \times\cos(\theta_{\tilde{u}\zeta}(f)-\theta_{\tilde{w}\zeta}(f)) \qquad (3.10)$$

The vertical profiles of T_1 and T_2 at the

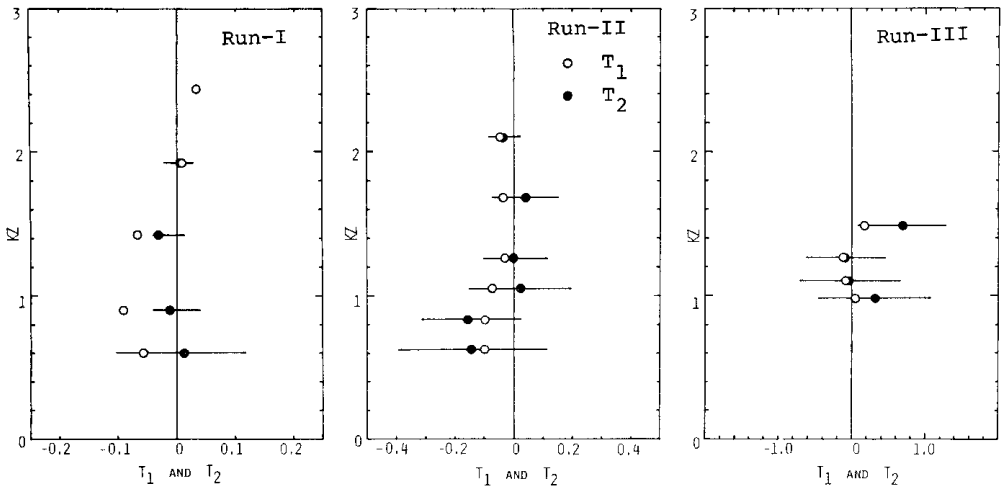

Fig. 7. Vertical profiles of the non-dimensional wave-induced Reynolds stresses T_1 (mark ○) and T_2 (mark ●) evaluated by two methods at the frequency f_p. The variable range of T_2 under the 95% confidence limit of the phase-difference is shown by the line through the closed circle.

wave spectral peak are shown in Fig. 7, where T_1 and T_2 are represented by an open and a closed circle, respectively. In this figure, the variable range of T_2 under the 95% confidence limit of the phase-difference is also shown. It is seen from this figure that the values of wave-induced Reynolds stress, obtained by the two methods described above, are similar with regard to the variation for the height above the mean water surface level.

This fact means that the two methods described above are appropriate to estimate the wave-induced Reynolds stress. From this figure, it is found that the values of the wave-induced Reynolds stress is negative at several heights over wind-waves. These experimental results are fairly different from the theoretical results given by Miles' inviscid quasi-laminar model. The negative value of the wave-induced Reynolds stress is an unexpected result. The same phenomena as shown in Fig. 7 have been found from the wind tunnel experiments over the regular waves by LAI and SHEMDIN (1971) and KATO and SANO (1971), and from the field observations by DAVIDSON *et al.* (1973). These phenomena are predicted theoretically by YEFIMOV (1970), DAVIS (1970) and TOWNSEND (1972), who took into account the turbulent shear flow over the wavy boundary. The present experimental situation differs from those in their experimental and theoretical studies; *i.e.*, in the present experiment, the critical layer for the dominant component wave of the irregular wind-wave field is lower than the wave-crests, and the scales of wind-waves are much smaller than those discussed by them. Therefore, the present experimental results can not be directly compared with their results. In the next section, the viscous Orr-Sommerfeld equation will be numerically integrated under the suitable conditions to the present wind tunnel experiment and the solutions will be compared with the experimental results.

4. Comparison between experimental and theoretical results

From the present experimental results, it is found that a wind-field over irregular wind waves has some characteristics different from the theoretical ones predicted by the Miles' (1957) quasi-laminar model. These differences will be attributed to the fact that the Miles' model did not take into account the atmospheric turbulence in the form of the wave-induced variations of turbulent Reynolds stresses proposed by PHILLIPS (1966).

The mechanism by which the wave-induced variations of turbulent Reynolds stresses are produced has not been clarified yet. In this article, we take into account the effect of the

atmospheric turbulence by introducing an eddy viscosity. We take the assumptions similar to those of Yefimov's (1970), as is described below.

1) The wave-induced variations of tangential turbulent Reynolds stress $\tilde{r}_{13}$ is represented as

$$\tilde{r}_{13}=\langle -u'w'\rangle-\langle -\overline{u'w'}\rangle =\nu_e\left(\frac{\partial}{\partial z}\tilde{u}+\frac{\partial}{\partial x}\tilde{w}\right) \qquad (4.1)$$

where ν_e is the kinematic eddy viscosity of the air. It is assumed that ν_e is independant of z and much greater than the kinematic molecular viscosity ν_m.

Here, the operator $\langle\ \rangle$ denotes an average over y, in the direction along the crests of the component wave, as same as that denoted by PHILLIPS (1966), and the over-bar denotes an average over several waves in the direction of the propagation of the component wave.

2) The wave-induced perturbations of the normal turbulent Reynolds stresses $\tilde{r}_{11}$ and $\tilde{r}_{33}$, defined by

$$\tilde{r}_{11}=\langle -u'^2\rangle-\overline{\langle -u'^2\rangle}$$
$$\tilde{r}_{33}=\langle -w'^2\rangle-\overline{\langle -w'^2\rangle}$$

respectively, are equal to each other.

3) The slope of a component wave is so small that the cross terms of the wave-induced velocity fluctuations in the equations of motion are negligible comparing with other terms.

4) A vertical profile of the mean wind velocity follows the logarithmic law in the turbulent boundary layer. As the air flow over the wind-waves is aerodynamically rough, the viscous sublayer does not exist, and therefore, the mean wind velocity becomes zero at a height lower than the roughness height. The wave-induced fluctuations of wind at the mean water surface level approximately represent the velocity fluctuations of water, *i.e.*, the wave-motion, at that level.

All variables are non-dimensionalized by taking k^{-1} and ω^{-1} as the scales of the length and the time, respectively. The wave-induced velocity fluctuations are non-dimensionalized by $a\omega$, where a is the amplitude of the component wave with the angular frequency ω.

From the assumptions 1, 2 and 3, the viscous Orr-Sommerfeld equation over a component wave is obtained as

$$(U-1)(\hat{\phi}''-\hat{\phi})-\hat{\phi}U''=\frac{-i}{Re}(\hat{\phi}^{\mathrm{IV}}+2\hat{\phi}''+\hat{\phi}) \qquad (4.2)$$

where the dash represents the differentiation about kz, and $Re(=\omega/\nu_e k^2)$ is the eddy viscous Reynolds number. $\hat{\phi}$ is the non-dimensional complex variable defined as

$$\tilde{\phi}=\frac{a\omega}{k}\,\Re\mathfrak{e}\,\{\hat{\phi}(kz)\exp(i(kx-\omega t))\} \qquad (4.3)$$

where $\tilde{\phi}$ is the stream function of the wave-induced velocity fluctuations of wind. U is the non-dimensional mean wind velocity non-dimensionalized by the phase velocity of the component wave and is given by

$$U=\begin{cases}\dfrac{U_0}{\kappa}\ln\left(\dfrac{kz}{z_0}\right), & kz>z_0\\ 0, & kz\leqq z_0\end{cases} \qquad (4.4)$$

from the assumption 4, where $U_0(=ku_*/\omega)$ is the non-dimensional friction velocity, z_0 the non-dimensional roughness parameter, and κ the Karman's constant. From the assumptions 1 and 2, it is found that the Eq. (4.2) differs from the ordinary Orr-Sommerfeld equation only in the sign of the term $2\hat{\phi}''$ on the right-hand side.

The boundary conditions are obtained from the assumption 4 as

$$\hat{\phi}(0)=1, \text{ and } \hat{\phi}'(0)=1 \qquad (4.5)$$

at the mean water surface level, and also

$$\hat{\phi}(H)=0, \text{ and } \hat{\phi}'(H)=0 \qquad (4.6)$$

at a sufficiently large height H at which the effect of the waves is negligible.

It must be mentioned here that the Eq. (4.2) is different from the equation derived by YEFIMOV (1970), who non-dimensionalized the mean wind velocity and the phase speed of the wave by $a\omega$, and that the sign of $\hat{\phi}'(0)$ is different from that used by YEFIMOV (1970) who took into account the effects of viscous sublayer.

In order to solve the Eq. (4.2) the value of ν_e is neccesary to be given. We have, however, no information about ν_e in the turbulent shear flow over the irregular wavy boundary. We have obtained the solutions for some values of ν_e from 1.5×10^1 to $1.5\times10^4\,\mathrm{cm^2\,s^{-1}}$, being

given the observed values of U_0 and z_0 corresponding to the component wave of the wave spectral peak. To compare the numerical solution with the experimental values $\sigma_{\tilde{u}}^2(f_p)$, $\sigma_{\tilde{w}}^2(f_p)$, $\theta_{\tilde{u}\zeta}(f_p)$, $\theta_{\tilde{w}\zeta}(f_p)$ and $T_1(f_p)$, we estimate the quantities σ_u^2, σ_w^2, θ_u, θ_w and T which correspond to the experimental values, respectively. They are expressed as follows:

$$\sigma_u^2=\frac{1}{2}|\hat{\phi}'|^2, \quad \sigma_w^2=\frac{1}{2}|\hat{\phi}|^2,$$

$$\theta_u=\arctan\,(-\hat{\phi}_i'/\hat{\phi}_r'), \quad \theta_w=\arctan\,(\hat{\phi}_r/\hat{\phi}_i),$$

$$T=-\frac{1}{2}\,\mathrm{Im}\,(\hat{\phi}\,\hat{\phi}_*') \qquad (4.7\sim4.11)$$

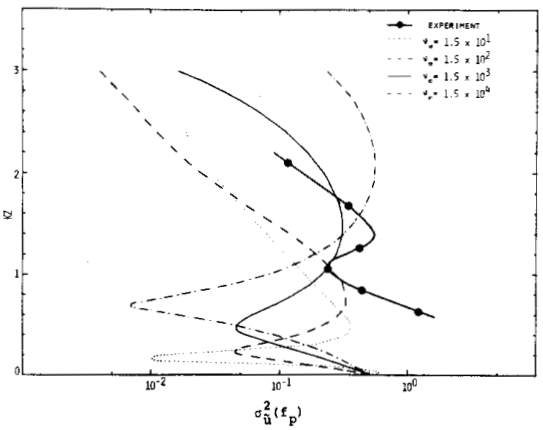

Fig. 8. Vertical profiles of σ_u^2 obtained from the numerical solutions of the Eq. (4.2) corresponding to Run-II, and those of observed value of $\sigma_{\tilde{u}}^2(f_p)$ in Run-II. The value of ν_e is in the range from 1.5×10^1 to 1.5×10^4 cm^2 s^{-1}.

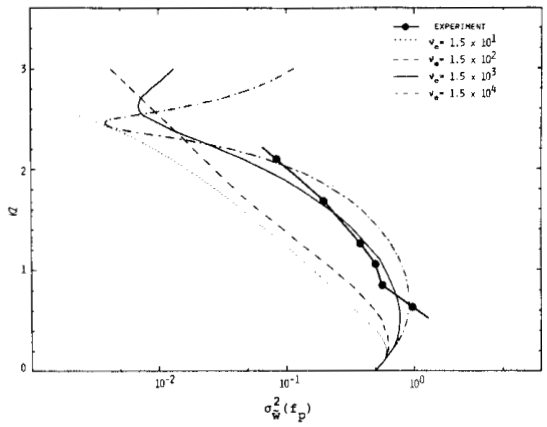

Fig. 9. Vertical profiles of σ_w^2 and $\sigma_{\tilde{w}}^2(f_p)$ in Run-II.

where the asterisk represents the complex conjugate, and suffixes r and i represent the real and imaginary parts, respectively.

The vertical profiles of σ_u^2, σ_w^2, θ_u, θ_w and T obtained from the numerical solutions of the Eq. (4.2), which correspond to Run-II of the experimental case, are shown in Figs. 8, 9, 10, 11 and 12, together with each measured one.

From Figs. 8 and 9, it is found that the vertical profiles of σ_u^2 and σ_w^2, obtained from the numerical solutions for an adequate value of ν_e, are qualitatively similar to the experimental profiles, although quantitative agreement is not sufficiently attained, for instance, the magnitude of σ_u^2 or σ_w^2 and the heights where σ_u^2 or σ_w^2 has a minimum value, are different. It can be seen from Fig. 12 that the vertical profile of the wave-induced Reynolds stress T

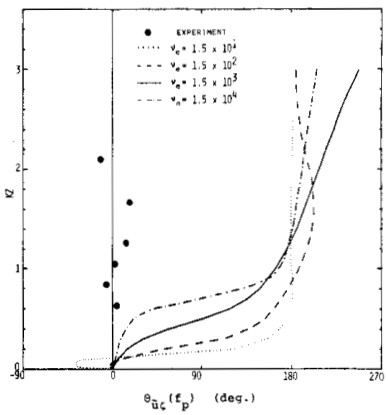

Fig. 10. Vertical profiles of θ_u and $\theta_{\tilde{u}\zeta}(f_p)$ in Run-II.

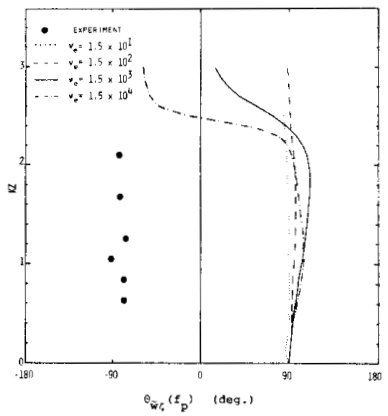

Fig. 11. Vertical profiles of θ_w and $\theta_{\tilde{w}\zeta}(f_p)$ in Run-II.

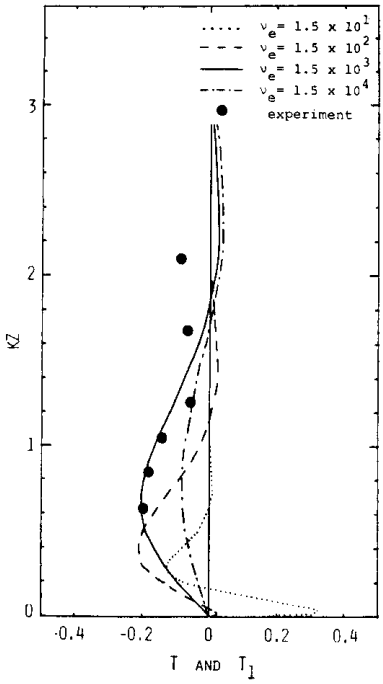

Fig. 12. Vertical profiles of T and $T_1(f_p)$ in Run-II.

obtained for an adequate value of ν_e is similar to the experimental results and the value of T is negative at several heights over the wavy boundary.

It is found, however, from Figs. 10 and 11 that the calculated phase-differences differ from the observed ones approximately by 180°. When Yefimov's boundary conditions are used instead of the Eq. (4.5), the similar discrepancy about the phase-differences also comes and the discrepancy in the magnitude of the wave-induced Reynolds stress is much greater than that in this article. The discrepancy about the phase-differences probably comes from the assumption about the boundary conditions at the water surface; *i.e.*, we adopt the assumption of the infinitesimal wave and give the boundary conditions at the mean water surface level, although the critical layer is lower than the wave-crests in this experimental case. The precise considerations about this problem will be made in the following paper.

Comparisons between the experimental and the theoretical results in the case of Run-I and Run-III are not mentioned in this paper. But they give the similar results to those of Run-II.

From the comparisons between the experimental results and the numerical solutions, it is concluded that the discrepancy between the observed wind field over wind-waves and the wind field expected from the inviscid quasi-laminar model can be attributed to the atmospheric turbulence, and that the theoretical model used in this article is not necessarily appropriate to predict the wind field over wind-waves.

5. Conclusion

For the wind field over the wind-waves in the wind tunnel the following conclusions are derived.

The measured vertical profiles of the power spectral density of the wave-induced velocity fluctuations of wind and the wave-induced Reynolds stress at the wave spectral peak frequency are different from the profiles expected from the inviscid quasi-laminar model. This difference may be attributed to atmospheric turbulence from the comparison between the experimental results and the numerical solutions of the viscous Orr-Sonmerfeld equation where the effects of the atmospheric turbulence is taken into account in the form of the eddy viscosity. It is considered that the atmospheric turbulence plays an important role in the momentum transfer from wind to wind-waves.

The theoretical model used in this article is, however, not necessarily appropriate to predict the wind field over wind-waves. The discrepancy between the experimental and the numerical results may come from the inadequate assumptions adopted in this study about the wave-induced variation of turbulent Reynolds stresses. It may also come from the assumption about the boundary conditions at the mean water surface level, *i.e.*, the assumption of the infinitesimal wave. Studies using a curve-linear coordinate are desirable.

Acknowledgements

The authors wish to express their thanks to Prof. Hideaki KUNISHI of Kyoto University for his discussion and encouragement. They also express their graditude to Mr. Kozaburo TANAKA for his assistance in carrying out the experiment, to Mrs. Yoko KIKUCHI for the data processing and to the Disaster Prevention Re-

search Institute, Kyoto University, for the use of the wind tunnel. The numerical calculations and the data processings in this article were carried out on a FACOM 230-75 in the Data Processing Center of Kyoto University. A part of this study was supported by scientific research fund from the Ministry of Education.

References

BARNETT, T. P. and J. C. WILKERSON (1967): On the generation of ocean wind waves as inferred from airborn radar measurements of fetch-limited spectra. J. Mar. Res., **25**, 292-328.

BLACKMANN, R. B. and J. W. TUKEY (1958): The Measurements of Power Spectra. Dover, New York, pp. 1-82.

DAVIDSON, K. L. and A. J. FRANK (1973): Wave-related fluctuations in the airflow above natural waves. J. Phys. Oceanogr., **3**, 102-119.

DAVIS, R.E. (1970): On the turbulent flow over a wavy boundary. J. Fluid Mech., **42**, 721-731.

DAVIS, R.E. (1972): On the prediction of the turbulent flow over a wavy boundary. J. Fluid Mech., **52**, 287-306.

HASSELMANN, K., T.P. BARNETT, E. BOUWS, H. CARLSON, D.E. CARTWRIGHT, K. ENKE, J.A. EWING, H. GIENAPP, D. E. HASSELMANN, P. KRUSEMAN, A. MEERBURG, P. MÜLLER, D.J. OLBERS, K. RICHTER, W. SELL and H. WALDEN (1973): Measurements of wind-wave growth and swell decay during the Joint North Sea Wave Project (JONSWAP). Ergänzungsheft zur Deutschen Hydrographischen Zeitschrift, Reihe A (8°), **12**, 1-95.

IMASATO, N. (1976a): Some characteristics of the development process of the wind-wave spectrum. J. Oceanogr. Soc. Japan, **32**, 21-32.

IMASATO, N. (1976b): The mechanism of the development of wind-wave spectra. J. Oceanogr. Soc. Japan, **32**, 253-266.

KAIMAL, J.C., J.C. WYNGAARD, Y. IZUMI and O. R. COTÉ (1972): Spectral characteristics of surface-layer turbulence. Q. J. Roy. Met. Soc., **98**, 563-589.

KATO, H. and K. SANO (1971): An experimental study of the turbulent structure of wind over water waves. Rep. of Port and Harbour Res. Inst., **10**, 3-42.

LAI, R. J. and O. H. SHEMDIN (1971): Laboratry investigation of air turbulence above simple water waves. J. Geophys. Res., **76**, 7334-7350.

LIGHTHILL, M.J. (1962): Physical interpretation of the mathematical theory of wave generation by wind. J. Fluid Mech., **14**, 385-398.

MILES, J.W. (1957): On the generation of surface waves by shear flows. J. Fluid Mech., **3**, 185-204.

MILES, J.W. (1962): On the generation of surface waves by shear flows. Part 4. J. Fluid Mech., **16**, 209-227.

MUNK, W.H. and D.E. CARTWRIGHT (1966): Tidal spectroscopy and prediction. Phil. Tras. Roy. Soc. A, **259**, 533-581.

PHILLIPS, O.M. (1958): The equibrium range in the spectra of wind waves. J. Fluid Mech., **2**, 417-445.

PHILLIPS, O.M. (1966): The Dynamics of the Upper Ocean. Cambridge Univ. Press, London, pp. 113.

REYNOLDS, W.C. and A. K. M. F. HUSSAIN (1972): The mechanics of an organized wave in turbulent shear flow. Part 3. Theoretical models and comparisons with experiments. J. Fluid Mech., **54**, 263-288.

SNYDER, R.L. and COX, C.S. (1966): A field study of the wind generation of ocean waves. J. Mar. Res., **24**, 141-178.

STEWART, R.H. (1970): Laboratry studies of the velocity field over deep-water waves. J. Fluid Mech., **42**, 733-754.

TOWNSEND, A.A. (1972): Flow in a deep turbulent boundary layer over a surface distorted by water waves. J. Fluid Mech., **55**, 719-735.

YEFIMOV, V.V. (1970): On the structure of the wind velocity field in the atmospheric near-water layer and the transfer of wind energy to sea waves. Izv. Atmos. Oceanic Physics., **6**, 1043-1053.

風波の上の風の場

市川　洋*，今里哲久*

要旨：風洞水槽でX型熱線風速計を用いて，風波の上の風速変動の鉛直分布を測定した．波のスペクトルピーク周波数 f_p をもつ波に誘起された風速変動のパワースペクトル密度 $S_{\tilde{u}}(f_p)$，$S_{\tilde{w}}(f_p)$ 及び wave-induced Reynolds stress—$C_{\tilde{u}\tilde{w}}(f_p)$ の鉛直分布は，非粘性準層流モデルによって予測される鉛直分布と異なり，wave-induced Reynolds stress は，ある高さでは負になっている場合がある．

このような相異は空中の乱流成分に起因しているということを，波の上の乱流シアーフローに関する線形モデルの数値解を求めて，実験結果と比較することによって示した．

* 京都大学理学部地球物理学教室，〒606 京都市左京区北白川追分町